Electronic Supporting Information

Amorphization of fused perylene diimide dimers for high-efficiency potassium-organic batteries

Mengyuan Cheng[a,b+], Hang Liu[a,b+], Zhuocheng Tian[a,b], Xiaoqi Luo[a,b], Di Wu[a,b], Kui Yan[a,c*] and Dongxue Wang[a,b*]

[a] School of Chemistry, Chemical Engineering and Life Science, Wuhan University of Technology, Wuhan 430070, P. R. China.

[b] State Key Laboratory of Advanced Technology for Materials Synthesis and Processing, Center of Smart Materials and Devices, Wuhan University of Technology, Wuhan 430070, P. R. China.

[c] International School of Materials Science and Engineering, Wuhan University of Technology, Wuhan 430070, P.R. China

*Corresponding Authors:

E-mail: ykui@whut.edu.cn, wangdongxue@whut.edu.cn

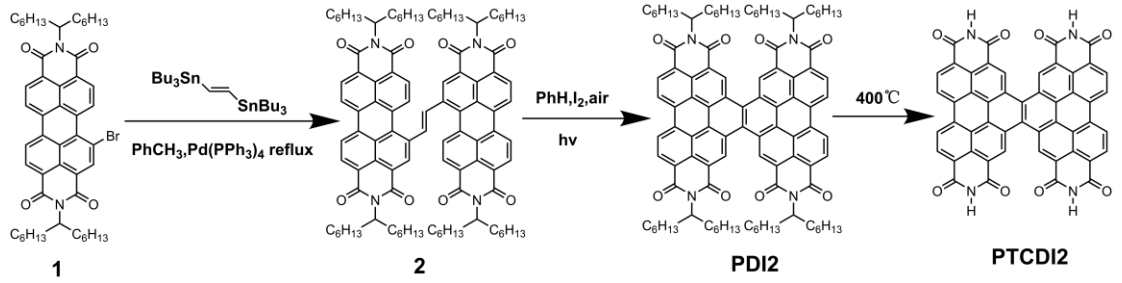

Scheme S1. Synthetic route of PTCDI2.

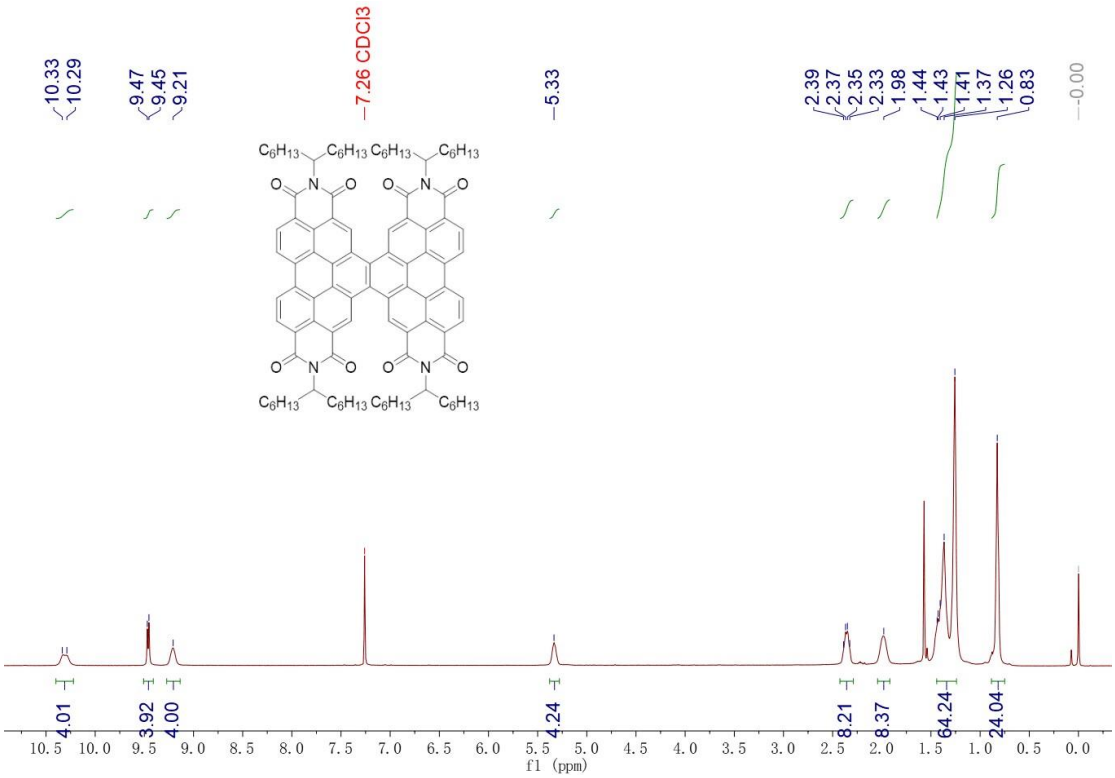

Figure S1. ^{1}H NMR spectra for PDI2.

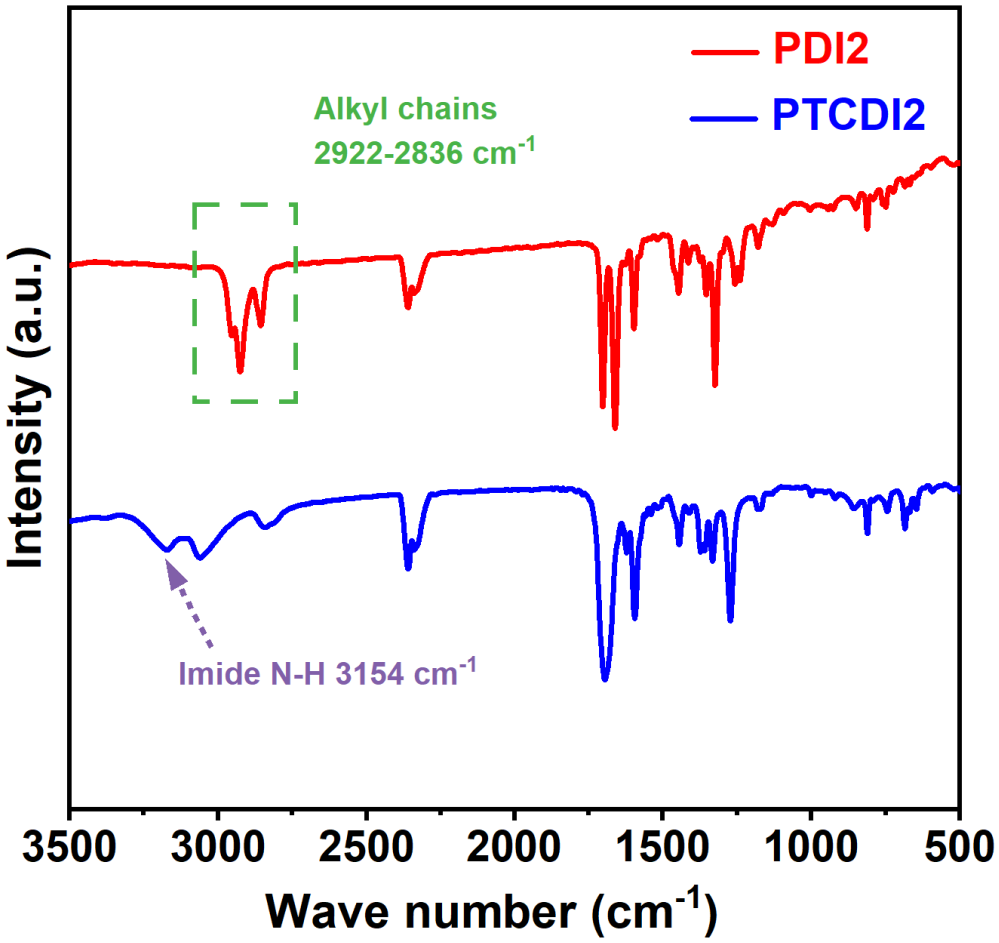

Figure S2. FTIR spectra of PDI2 and PTCDI2.

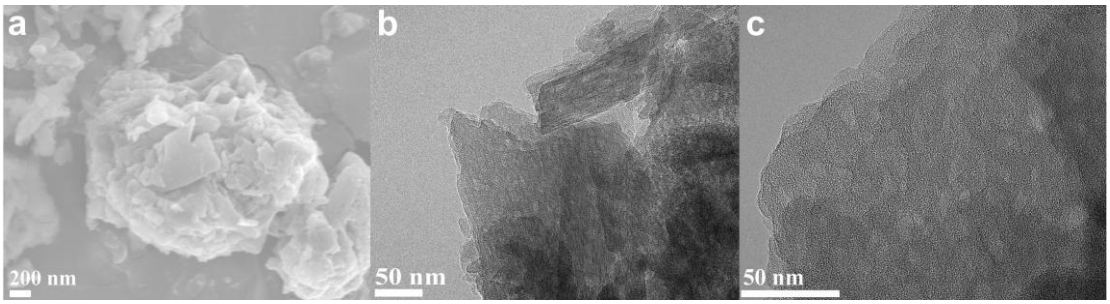

Figure S3. (a) SEM, (b, c) TEM images of PTCDI2.

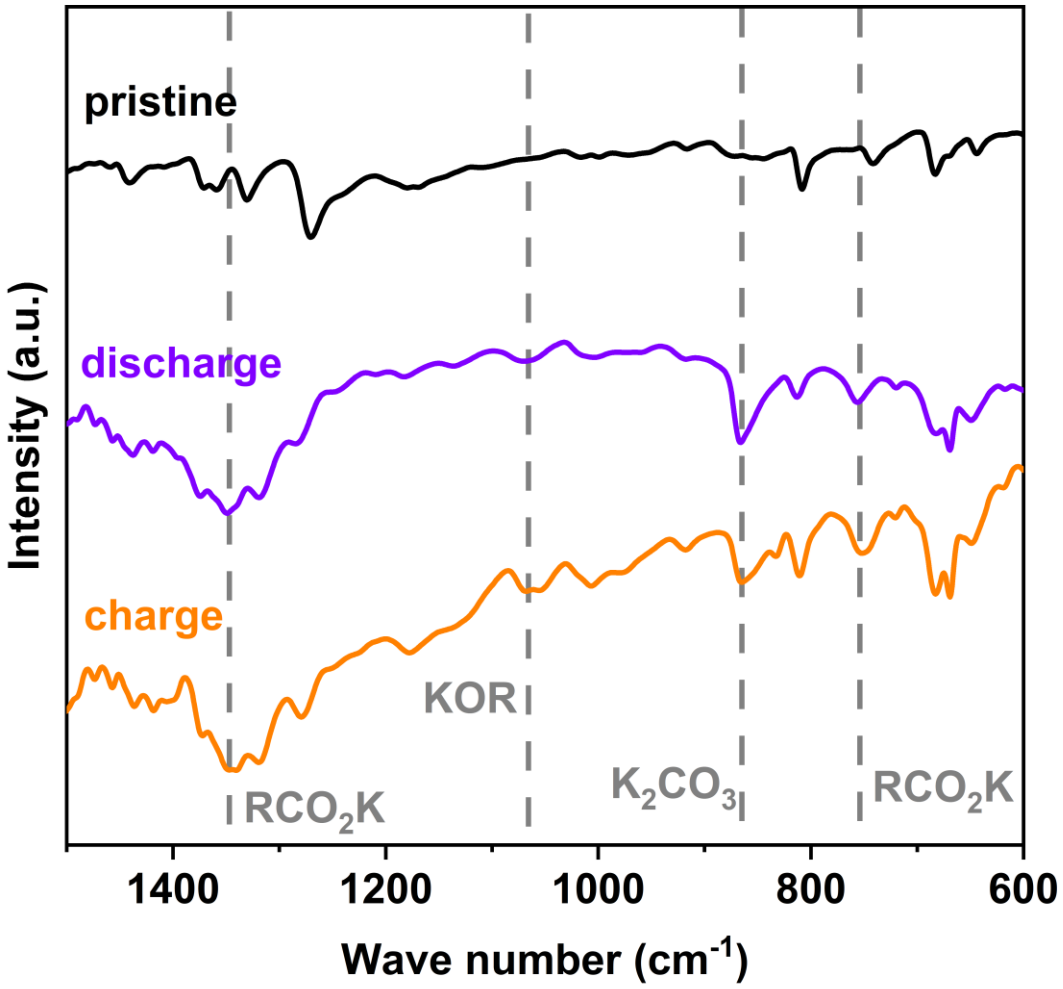

Figure S4. *Ex-situ* FTIR of PTCDI2 anodes.

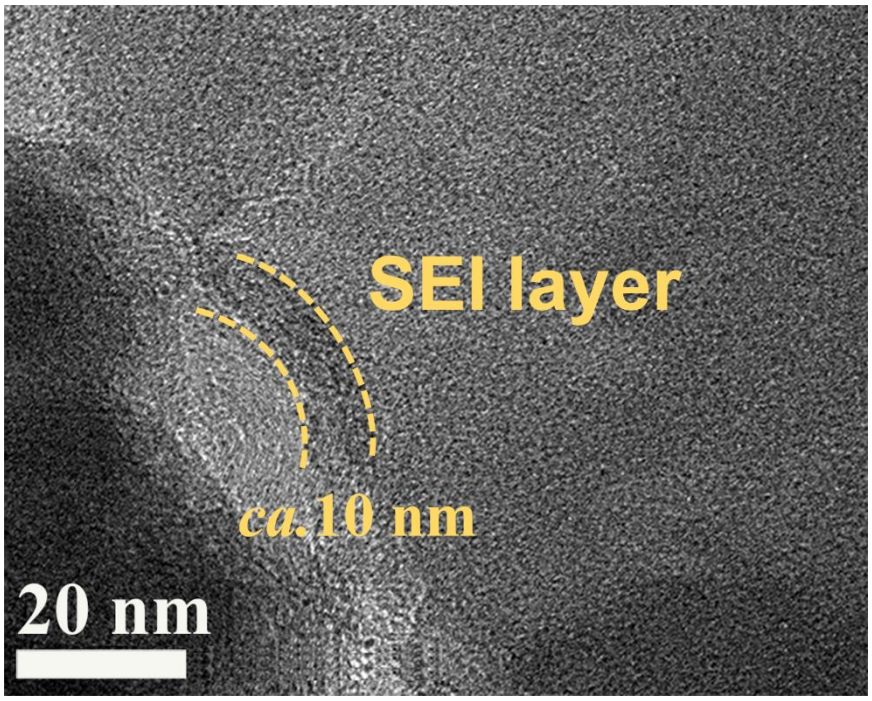

Figure S5. HRTEM image of PTCDI2 after the initial cycle.

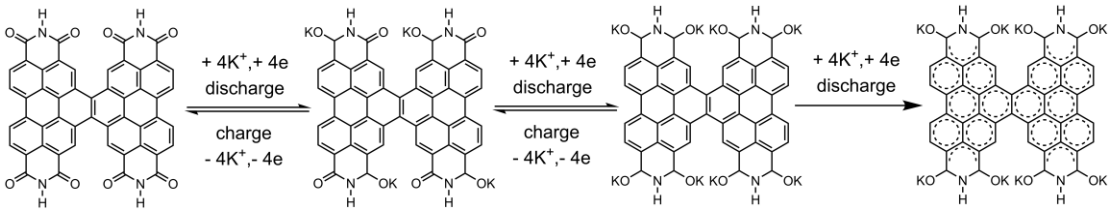

Scheme S2. Possible eight-electron storage mechanism for PTCDI2.

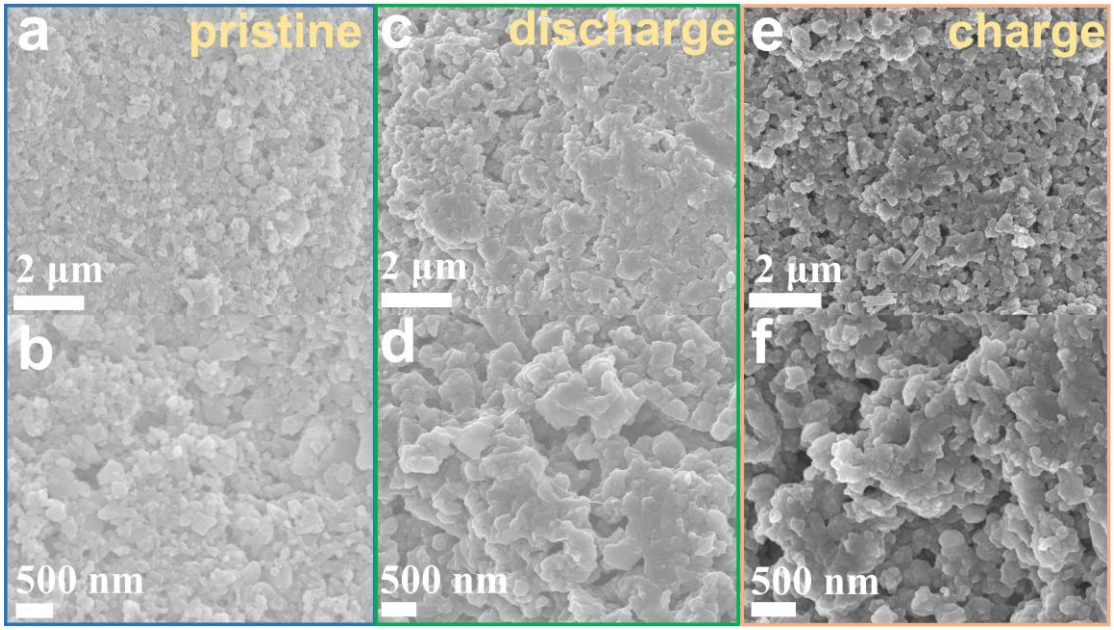

Figure S6. The SEM images of PTCDI2 electrode at (a, b) pristine, (c, d) fully discharged and (e, f) fully charged state.

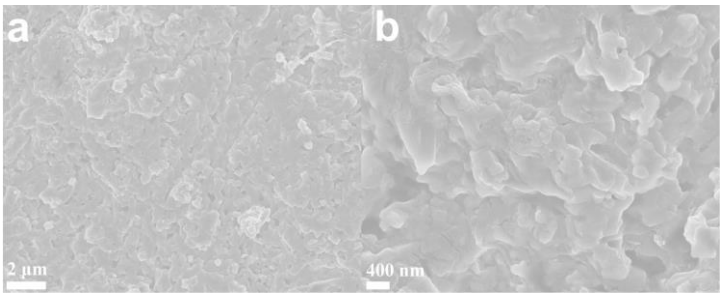

Figure S7. (a, b) The SEM images of PTCDI2 electrode after long cycle at different scale bars.

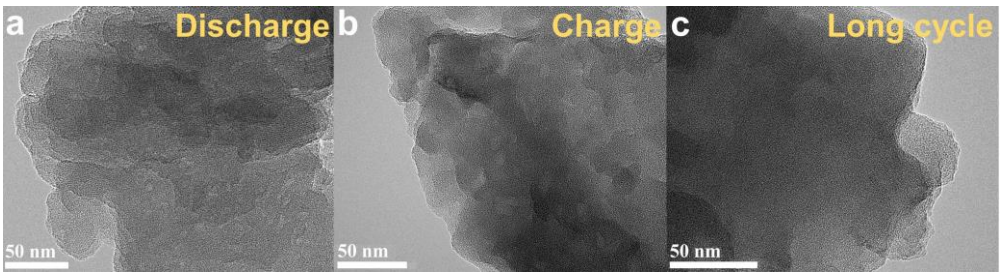

Figure S8. The TEM images of PTCDI2 electrode at the fully discharged (a) fully recharged (b) and long cycle (c) states.

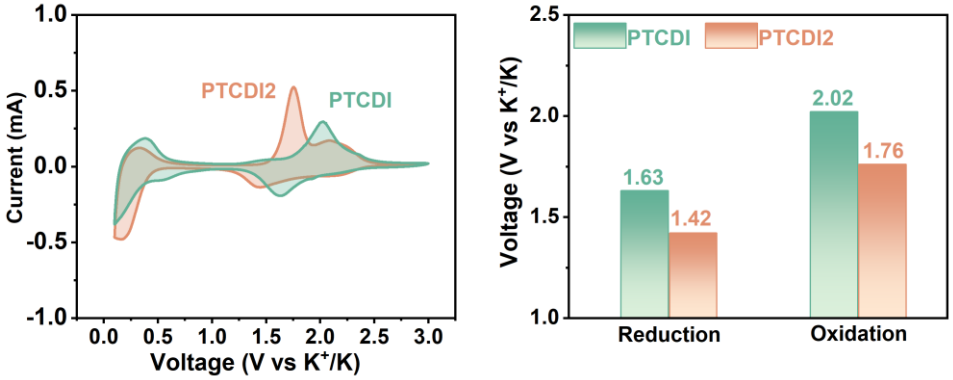

Figure S9. (a) CV curves of PTCDI2 and PTCDI at 0.5 mV s^{-1}, (b) the average oxidation and reduction potential comparison picture of PTCDI2 and PTCDI.

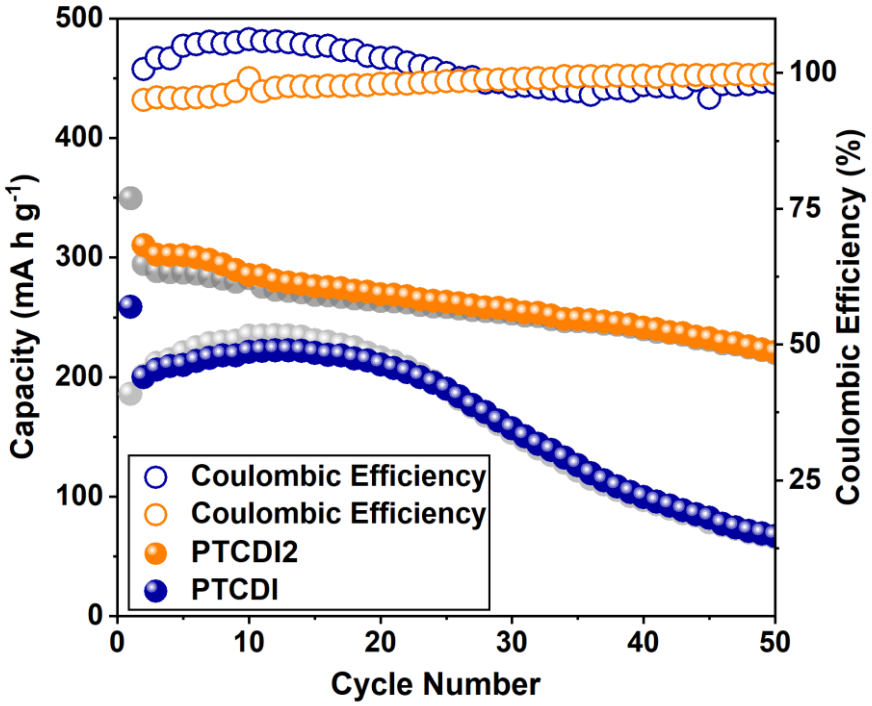

Figure S10. The cycle performance of PTCDI2 and PTCDI at the current density of 0.5 A g^{-1}.

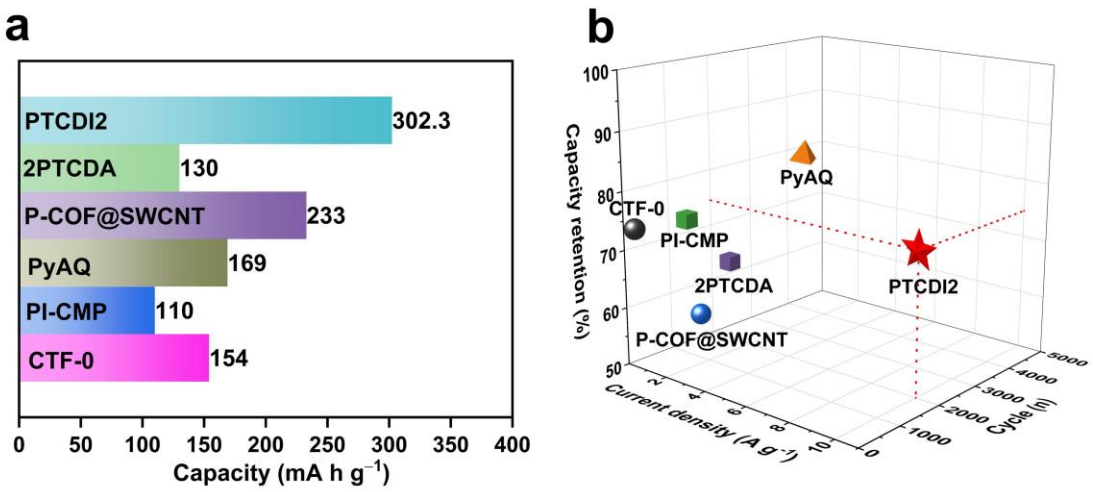

Figure S11. (a) The reversible capacity and (b) cyclic stability of PTCDI2 compared with some representative organic PIBs.

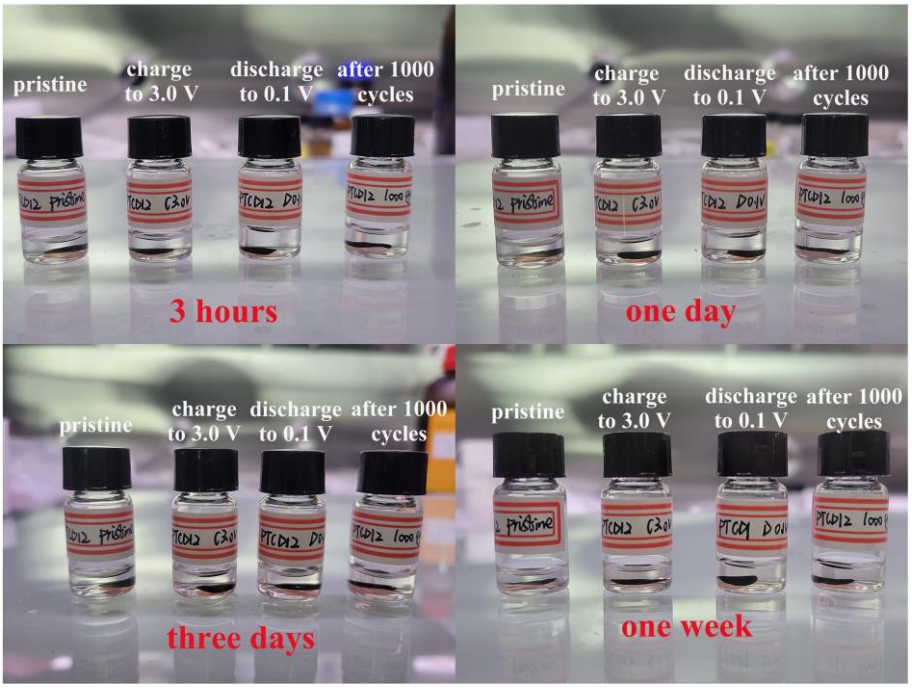

Figure S12. The solubility test of PTCDI2 at various states: pristine, charged to 3.0 V, discharged to 0.1 V and after 1000 cycles at the current density of 10 A g^{-1}.

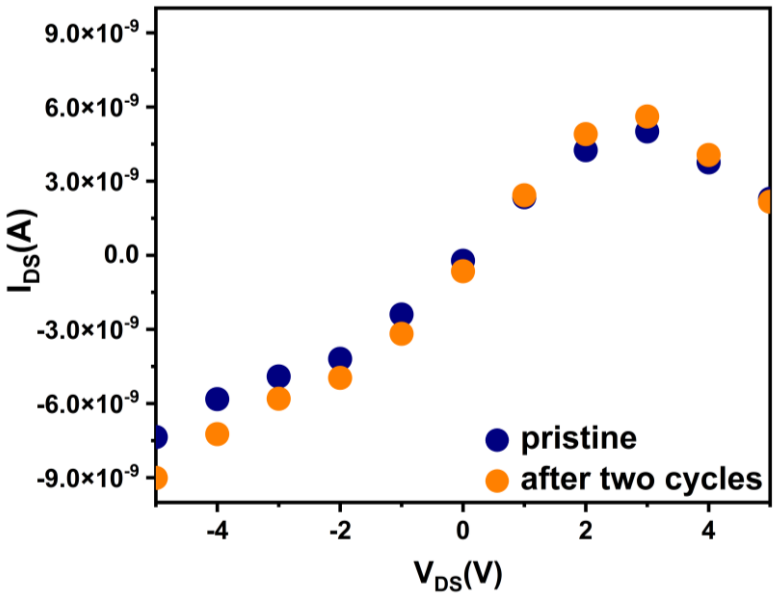

Figure S13. I-V plots of PTCDI2 at different stages.

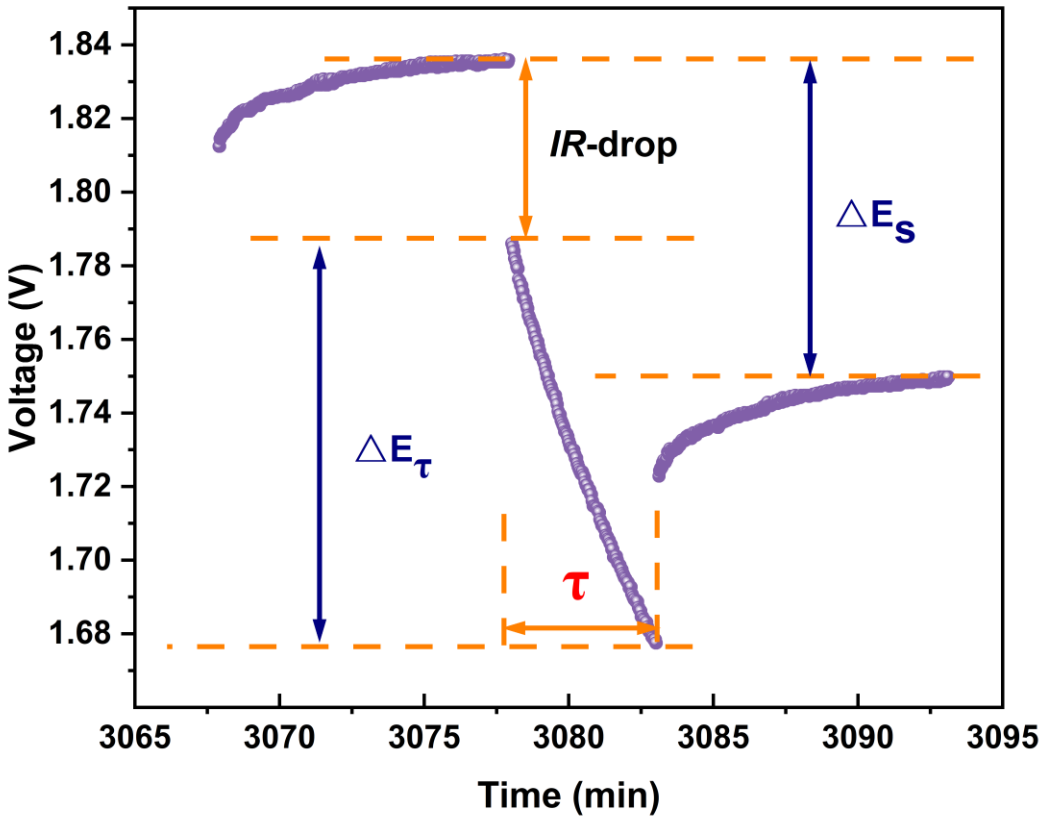

Figure S14. GITT potential response curve with time for one typical discharge step of PTCDI2.

The galvanostatic intermittent titration technique (GITT) was carried out to study the charge transfer kinetics of the PTCDI2 electrodes. The GITT data was conducted with a current pulse at 100 mA g^{-1} for 10 min and rest intervals for 5 min. The K-ions diffusion coefficients can be calculated through the Equation (1) [S1, S2]:

$$\widetilde{D} = \frac{4}{\pi}\left(\frac{m_B V_M}{M_B S}\right)^2 \left(\frac{\Delta E_s}{\tau\left(\frac{dE_\tau}{d\sqrt{\tau}}\right)}\right)^2 \left(\tau \ll \frac{L^2}{D}\right) \approx \frac{4}{\pi\tau}\left(\frac{m_B V_M}{M_B S}\right)^2 \left(\frac{\Delta E_s}{\Delta E_\tau}\right)^2 \quad (1)$$

In this equation, m_B is the loading mass of active materials, V_M is the molar volume, M_B is the molar weight of PTCDI2, S is the active surface area of the electrode (0.5 cm^2), τ is the relaxation time (300 s). $\Delta E\tau$ and ΔEs are the total change in the cell voltage during the current pulse and the change in the stationary voltage of the cell during the plateau potential step, respectively, schemed in Figure S14.

In this experiment, m_B/M_B equals to the n_B, which can be calculated through the Equation (2)[S3]:

$$\frac{m_B V_M}{M_B S} = \frac{n_B V_M}{S} = L \quad (2)$$

The K-ion diffusion coefficients can be calculated through the simplified Equation (3):

$$\widetilde{D} \approx \frac{4}{\pi\tau}(L)^2 \left(\frac{\Delta E_S}{\Delta E_\tau}\right)^2 \quad (3)$$

SEM image shown in Figure S15 was used to confirm the average thickness (*L*) of PTCDI2.

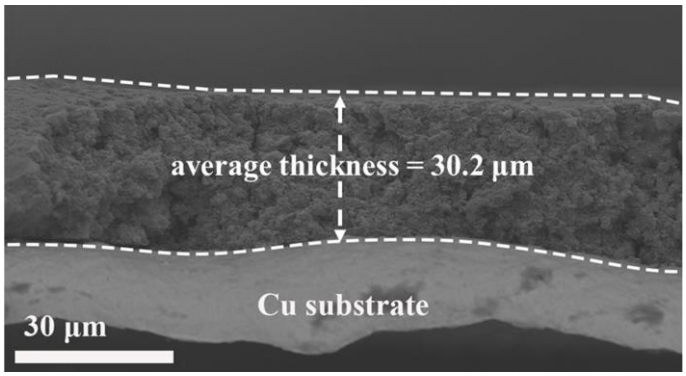

Figure S15. The thickness of PTCDI2 electrode.

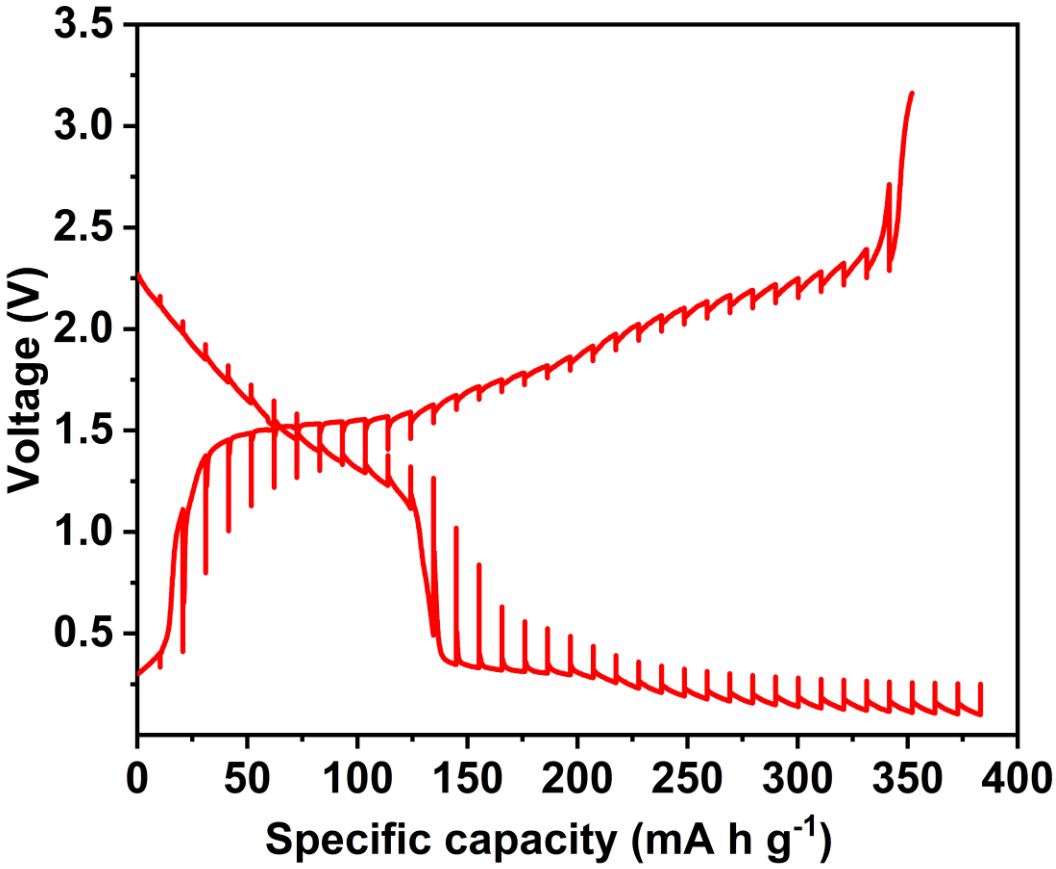

Figure S16. GITT curves of PTCDI2 in the third charge/discharge cycle.

Table S1. The detailed intensity comparison table for all relevant peaks.

Detailed intensity comparison	pristine	discharge	charge
C–C	62.99 %	27.18 %	35.46 %
C=C	17.56 %	39.11 %	39.76 %
C–N	8.35 %	8.18 %	4.12 %
C=O	11.10 %	1.42 %	7.64 %
C–O	-	15.51 %	4.18 %
O-C=O	-	8.59 %	8.83 %

Table S2. The long-term cyclic life compared with reported organic anodes in PIBs.

Anode	Current ($A\ g^{-1}$)	Initial capacity ($mA\ h\ g^{-1}$)	Cycle Number(n)	Capacity retention (%)
This work	**10**	**141**	**2000**	**74.5**
PTCDI [S4]	5	218	320	90.3
K2TP [S5]	1	205	500	94.6
K2BPDC@GR [S6]	1	147	3000	40.8
HAT-COOK [S7]	0.5	235	500	63.8
PI-1[S8]	1	201	200	95.6
COF-10@CNT [S9]	1	281	4000	57.3
P-COF@SWCNT [S10]	0.7	204	1400	55.8
CTF-1 [S11]	0.1	68	300	82.3

Table S3. EIS fitting data of PTCDI2 based on equivalent circuit.

	1st	2nd
R_{SEI}	52.4 Ω	63.6 Ω
R_{ct}	219.8 Ω	92.6 Ω

Refs:

S1. Z. Xing, Z. Jian, W. Luo, Y. Qi, C. Bommier, E. S. Chong, Z. Li, L. Hu and X. Ji, *Energy Environ. Sci.*, 2016, **2**, 63-68.

S2. Z. Wei, D. Wang, M. Li, Y. Gao, C. Wang, G. Chen and F. Du, *Adv. Energy Mater.*, 2018, **8**, 1801102.

S3. Y. Hu, W. Tang, Q. Yu, X. Wang, W. Liu, J. Hu and C. Fan, *Adv. Funct. Mater*. , 2020, **30**, 2000675.

S4. Y. Bai, W. Fu, W. Chen, Z. Chen, X. Pan, X. Lv, J. Wu and X. Pan, *J. Mater. Chem. A*., 2019, **7**, 24454-24461.

S5. Lei, F. Li, C. Mu, J. Wang, Q. Zhao, C. Chen and J. Chen, *Energy Environ. Sci.*, 2017, **10**, 552-557.

S6. C. Li, Q. Deng, H. Tan, C. Wang, C. Fan, J. Pei, B. Cao, Z. Wang and J. Li, *ACS Appl. Mater. Interfaces*., 2017, **9**, 27414-27420.

S7. J. Zou, C. Fu, Y. Zhang, K. Fan, Y. Chen, C. Zhang, G. Zhang, H. Dai, Y. Cao and J. Ma, *Adv. Funct. Mater.*, 2023, 33, 2303678.

S8. R. R. Kapaev, I. S. Zhidkov, E. Z. Kurmaev, K. J. Stevenson and P. A. Troshin, *Chem. Comm*., 2020, **56**, 1541-1544.

S9. X. Chen, H. Zhang, C. Ci, W. Sun and Y. Wang, *ACS nano*., 2019, **13**, 3600-3607.

S10. X. X. Luo, W. H. Li, H. J. Liang, H. X. Zhang, K. D. Du, X. T. Wang, X. F. Liu, J. P. Zhang and X. L. Wu, *Angew. Chem.-Int. Edit.*, 2022, **134**, e202117661.

S11. S.-Y. Li, W.-H. Li, X.-L. Wu, Y. Tian, J. Yue and G. Zhu, *Chem. Sci.*, 2019, **10**, 7695-7701.